

# Functional Expression of Geraniol 10-Hydroxylase Reveals Its Dual Function in the Biosynthesis of Terpenoid and Phenylpropanoid

Pin-Hui Sung,<sup>||</sup> Fong-Chin Huang,<sup>S,||</sup> Yi-Yin Do,\* and Pung-Ling Huang\*

Department of Horticulture, National Taiwan University, No. 1 Roosevelt Road, Section 4, Taipei 10617, Taiwan, Republic of China

**ABSTRACT:** Geraniol 10-hydroxylase (G10H), a cytochrome P450 monooxygenase, has been reported to be involved in the biosynthesis of terpenoid indole alkaloids. The gene for *Catharanthus roseus* G10H (*CrG10H*) was cloned and heterologously expressed in baculovirus-infected insect cells. A number of substrates were subjected to assay the enzyme activity of CrG10H. As reported in a previous study, CrG10H hydroxylated the monoterpene geraniol at the C-10 position to generate 10-hydroxygeraniol. Interestingly, CrG10H also catalyzed 3'-hydroxylation of naringenin to produce eriodictyol. Coexpression of an *Arabidopsis* NADPH P450 reductase substantially increased the ability of CrG10H to hydroxylate naringenin. The catalytic activity of CrG10H was approximately 10 times more efficient with geraniol than with naringenin, judged by the  $k_{cat}/K_m$  values. Thus, G10H also plays an important role in the biosynthetic pathway of flavonoids, in addition to its previously described role in the metabolism of terpenoids.

**KEYWORDS:** *Catharanthus roseus*, geraniol 10-hydroxylase, cytochrome P450 reductase, secondary metabolism, baculovirus system

## INTRODUCTION

*Catharanthus roseus* (Madagascar periwinkle) is an important natural source of terpenoid indole alkaloids (TIAs), which produce a diverse group of pharmaceutically important molecules. Prominent among these are the effective anticancer agents vincristine and vinblastine. However, these alkaloids exist at extremely low levels within the plants, and chemical synthesis is not feasible due to their complex structures.<sup>1</sup>

TIAs are synthesized from the condensation of tryptamine and secologanin. Tryptamine is derived from tryptophan by tryptophan decarboxylase, whereas secologanin is derived from geranyl pyrophosphate. The condensation of tryptamine and secologanin is catalyzed by strictosidine synthase (STR), and the product strictosidine is converted to cathenamine, a precursor to various active alkaloids, by strictosidine glucosidase (SGD). To date, several key enzymes involved in TIA biosynthesis have been isolated and characterized, and the genes encoding some of these enzymes have been cloned.<sup>2</sup> Figure 1 shows the biosynthetic pathway of TIAs. Geraniol 10-hydroxylase (G10H) catalyzes the first committed step in the pathway.<sup>2</sup>

In *C. roseus*, CrG10H (a cytochrome P450 monooxygenase belonging to the CYP76B superfamily) has been suggested to be a potential site for regulation of secologanin production. Previous studies also showed that increased *CrG10H* gene transcripts and enzyme activity have been associated with the increased accumulation of TIAs.<sup>2–4</sup>

The biological functions of P450s rely on an electron donor, NADPH-cytochrome P450 reductase (CPR). CPR transfers two electrons from NADPH to P450s.<sup>5</sup> Due to the low abundance of P450s and the many difficulties encountered in fractionating individual proteins from endogenous P450s pools, more recent approaches for the characterization of P450s rely on heterologous expression in a eukaryotic system. The use of eukaryotic systems allows P450 enzyme activities to be defined in cell lysates or purified microsomes together with an endogenous P450 reductase or a coexpressed P450 reductase.<sup>6</sup>

To investigate the biochemical role of CrG10H in the metabolism of phenylpropanoid and to establish a eukaryotic expression model system for *CrG10H* expression, we coexpressed *C. roseus* G10H (*CrG10H*) and a P450 reductase from *Arabidopsis* (*AtCPR1*) in insect cells. A variety of flavonoid substrates were subjected to the enzyme assay. Surprisingly, CrG10H exhibited not only geraniol 10-hydroxylase but also flavonoid 3'-hydroxylase activity in a reconstituted system containing NADPH:cytochrome P450 reductase. This is the first paper that ascribes G10H to be associated with the biosynthetic pathway of flavonoids. These findings suggest that G10H plays an important role in both terpenoid and flavonoid metabolism. The aim of this research is to reveal the potential of CrG10H dual function on the applied aspects of terpenoid and phenylpropanoid pathways.

## MATERIALS AND METHODS

**Chemicals.** Naringenin, eriodictyol, geraniol, apigenin, kaempferol, *p*-coumaric acid, ferulic acid,  $\beta$ -nicotinamide adenine dinucleotide 2'-phosphate reduced tetrasodium salt hydrate (NADPH), and  $\beta$ -nicotinamide adenine dinucleotide phosphate (NADP) were purchased from Sigma-Aldrich (St. Louis, MO). HPLC solvents were from J. T. Baker Inc. (Phillipsburg, NJ). All other chemicals were of the highest purity available. Organic solvents were of HPLC grade.

**Construction and Expression in Insect Cells.** The coding regions of *CrG10H* (GenBank accession no. AJ251269) and *AtCPR1* (GenBank accession no. X66016) were amplified by RT-PCR from first-strand cDNAs synthesized from total RNAs of leaves of *C. roseus* and *Arabidopsis thaliana*, respectively. The PCR primers used for *CrG10H* were CrG10H-S (5'-GACAGATCTATGGATTACCTTACCATAA-3', forward) and CrG10H-AS (5'-TGCTCTAGATTAAGGGTGCTTGGTACA-3', reverse), whereas for *AtCPR1* we used

**Received:** January 19, 2011

**Revised:** March 25, 2011

**Accepted:** March 27, 2011

**Published:** April 19, 2011

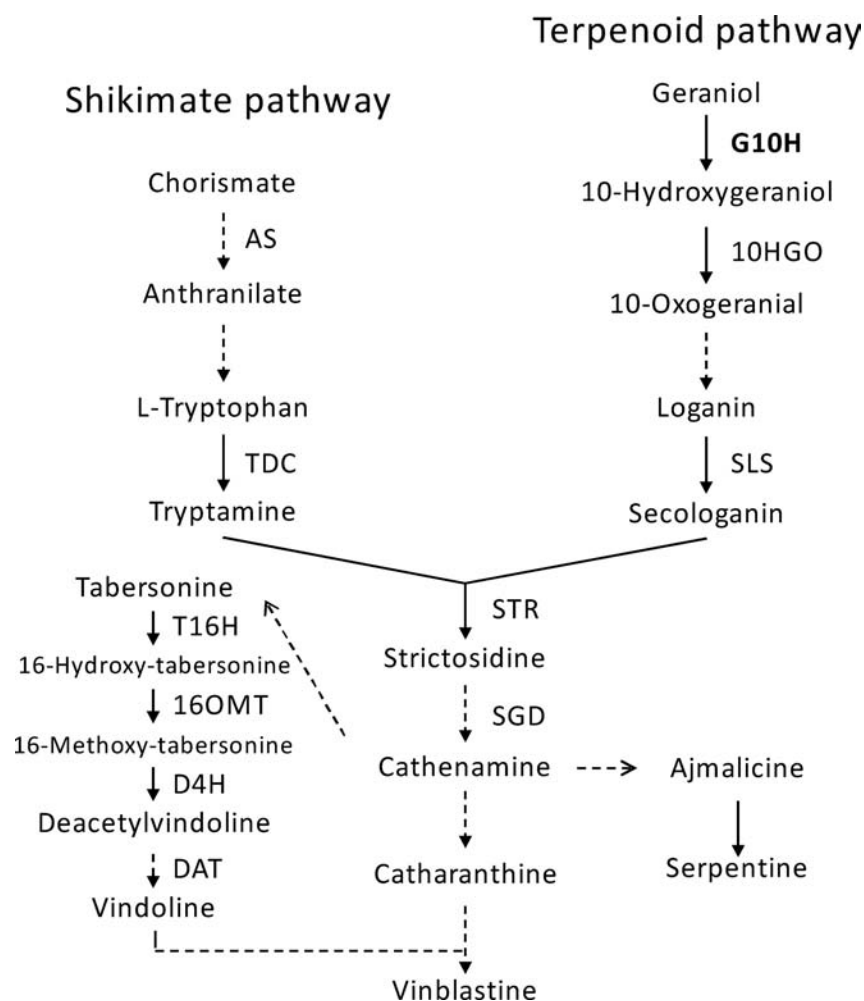


**Figure 1.** Schematic representation of the biosynthetic pathway of strictosidine and other terpenoid indole alkaloids (TIAs). Geraniol 10-hydroxylase (G10H), which catalyzes the first committed step of this pathway,<sup>2</sup> is highlighted in bold. Thin and dashed arrows represent single and multiple enzymatic steps, respectively. AS, anthranilate synthase; TDC, tryptophan decarboxylase; SLS, secologanin synthase; 10HGO, 10-hydroxygeraniol oxidoreductase; STR, strictosidine synthase; SGD, strictosidine  $\beta$ -glucosidase; T16H, tabersonine-16-hydroxylase; 16OMT, 16-hydroxytabersonine-*O*-methyltransferase; D4H, desacetoxyvindoline 4-hydroxylase; DAT, deacetylvindoline 4-*O*-acetyl transferase.

AtCPR1-S (*S'*-GACAGATCTATGACTTCTGCTTTGTAT-3', forward) and AtCPR1-AS (*S'*-CCGGAATTCTCACCAGACATCTCTGAG-3', reverse). The resulting PCR product of *CrG10H* was digested with *Bgl*II and *Xba*I and ligated with *Bam*HI/*Xba*I digested pFastBac1 vector (Invitrogen, Carlsbad, CA), whereas that of *AtCPR1* was digested with *Bgl*II and *Eco*RI and then ligated with the pFastBac1 vector, which was digested with *Bam*HI and *Eco*RI. The recombinant genes were subjected to sequencing to confirm the sequence of the inserts. The correct constructs were transposed into baculovirus DNA in the *Escherichia coli* strain DH10BAC (Invitrogen) and then transfected into *Spodoptera frugiperda* 9 (Sf9) cells according to the manufacturer's instructions (Invitrogen). The insect cells were propagated and the recombinant virus was amplified as described by Kraus and Kutchan.<sup>7</sup> For coexpression, recombinant baculovirus containing *CrG10H* was added simultaneously to Sf9 cells with recombinant virus containing *AtCPR1*.

**Detection of Recombinant CrG10H and AtCPR1 Genes in Insect Cells.** PCR analysis was used to detect recombinant baculovirus containing *CrG10H* or *AtCPR1* in insect cells. Insect cells infected with recombinant baculoviruses were collected by centrifugation and were then resuspended in solution I (15 mM Tris-HCl, pH 8.0, 10 mM EDTA, 100  $\mu$ g/mL RNase A). Then the cells were hydrolyzed for 5 min by adding an equal volume of solution II (0.2 N NaOH, 1% SDS),

followed by mixing with a half volume of solution III (3 M potassium acetate, pH 5.5) and incubation on ice for 5 min. After centrifugation (15000g for 10 min at room temperature), the supernatant was transferred to a new tube containing an equal volume of isopropanol. The recombinant DNA was pelleted by centrifugation (15000g for 5 min at room temperature) and dissolved in TE buffer (10 mM Tris-HCl, pH 8.0, 1 mM EDTA). The recombinant DNA was analyzed by PCR. The PCR condition for detection of *CrG10H* was 1 cycle of 94 °C for 2 min; 35 cycles of 94 °C for 45 s, 58 °C for 45 s, and 72 °C for 2 min; 1 cycle of 72 °C for 10 min using primers CrG10H-S and M13 reverse (*S'*-CAATTT-CACACAGGA-3'). That for detection of *AtCPR1* was 1 cycle of 94 °C for 2 min; 35 cycles of 94 °C for 45 s, 60 °C for 45 s, and 72 °C for 2 min; 1 cycle of 72 °C for 10 min using primers AtCPR1-S and M13 reverse.

**Quantification of CrG10H Protein.** Isolation of insect cell microsomes was performed as described.<sup>7</sup> For reduced CO difference analysis<sup>8</sup> of the CrG10H content in each sample, microsomal proteins were diluted in 2 mL of suspension buffer (100 mM Tricine buffer, pH 8.0, 5 mM thioglycolic acid), reduced with 2 mg of sodium dithionite, and divided into two cuvettes (1 cm path length). Subsequently, one cuvette was scanned from 400 to 500 nm for baseline, the sample cuvette was saturated with CO, and the difference spectra were recorded by comparison with the reduced baseline scan. CrG10H content was

calculated as  $(OD_{450} - OD_{490})/0.091/\text{mg} = \text{mmol of CrG10H}/\text{mg of microsomal protein}$ .

**Enzyme Activity Assays.** CrG10H enzyme activity was determined in 100  $\mu\text{L}$  of 200 mM Tricine buffer, pH 8.0, containing 250  $\mu\text{g}$  of microsomal protein, 500  $\mu\text{M}$  NADPH, and 100  $\mu\text{M}$  substrate. After incubation at 30 °C for 1 h, 20  $\mu\text{L}$  of 20% trichloroacetic acid (TCA) was added to stop the reaction. After removal of insoluble cell debris by centrifugation (15000g, 2 min at room temperature), the enzyme reaction was analyzed by GC-MS and HPLC-DAD system.

The enzyme reaction with geraniol was analyzed by gas chromatography–mass spectrometry (GC-MS), a Micromass Quattro Micro tandem quadrupole mass spectrometer run in selected ion monitoring (SIM) mode by electron impact ionization. The assay product dissolved in ethanol was separated on an Agilent 6890N gas chromatograph equipped with a DB-5 capillary column (30 m  $\times$  0.25 mm, film thickness of 0.25  $\mu\text{m}$ ) (J&W Scientific) using helium as carrier gas at a flow rate of 1.2 mL  $\text{min}^{-1}$ . The separation conditions were as follows: injection split ratio, 1:50; injector temperature, 250 °C; initial oven temperature, 50 °C for 0.5 min followed by a linear gradient to 300 °C at a rate of 10 °C  $\text{min}^{-1}$ . The mass scan range was  $m/z$  50–300 Da with a scan range time of 1 s.

The enzyme reactions with naringenin, apigenin, kaempferol, *p*-coumaric acid, and ferulic acid were analyzed by a HPLC-DAD system (autosampler, L-2200; binary pump, L-2130; diode array detector, L-2450; Hitachi, Tokyo). HPLC separations were performed on a reverse phase column (Mightysil-RP18, 5  $\mu\text{m}$ , 250  $\times$  4.6 mm, Kanto Chemical, Tokyo, Japan) and the following solvent system: (A) 97.99% (v/v)  $\text{H}_2\text{O}$ , 2%  $\text{CH}_3\text{CN}$ , 0.01% (v/v)  $\text{H}_3\text{PO}_4$ ; (B) 1.99% (v/v)  $\text{H}_2\text{O}$ , 98%  $\text{CH}_3\text{CN}$ , 0.01%  $\text{H}_3\text{PO}_4$ . The gradient was as follows: 0–25 min, 0–45% B; 25–26 min, 45–100% B; 26–30 min, 100–0% B; then hold for 2 min. The flow rate was 1 mL  $\text{min}^{-1}$ , and the detection wavelength was 284 nm.

**Kinetic Analysis.** For determination of the kinetic parameters for naringenin, the incubation mixture contained 200 mM Tricine buffer, pH 8.0, 250  $\mu\text{g}$  of microsomal protein (CrG10G and AtCPR1 coexpressed), 500  $\mu\text{M}$  NADPH, and various concentrations of naringenin (0, 5, 10, 50, 100, 200, and 400  $\mu\text{M}$ ) in a final volume of 100  $\mu\text{L}$ . Each reaction was allowed to proceed linearly for 30 min at 30 °C and was terminated by adding 20% TCA. The enzymatic product (eriodictyol) was quantified by HPLC using a standard curve calculated with various known concentrations of authentic eriodictyol (triplicate). The kinetic parameters ( $K_m$  and  $V_{\text{max}}$ ) were estimated by nonlinear regression with GraphPad Prism 5 (GraphPad software) in three independent experiments.

For determination of kinetic parameters for geraniol, the incubation mixture contained 200 mM Tricine buffer, pH 8.0, 250  $\mu\text{g}$  of microsomal protein (CrG10G and AtCPR1 coexpressed), 500  $\mu\text{M}$  NADPH, and various concentrations of geraniol (0, 5, 10, 15, 20, 25, and 50  $\mu\text{M}$ ) in a final volume of 100  $\mu\text{L}$ . Each reaction was allowed to proceed linearly for 30 min at 30 °C and was terminated by the addition of an equal volume of ethyl acetate. After mixing and centrifugation at 200g for 1 min, the ethyl acetate fraction was evaporated to dryness at room temperature using a vacuum concentrator. The residue was dissolved in 100  $\mu\text{L}$  of methanol and analyzed by GC-MS in full scan spectra. The enzymatic product (10-hydroxygeraniol) was quantified by GC-MS in full scan spectra using a standard curve calculated with various known concentrations of authentic geraniol (triplicate).

**Product Identification.** For analysis of CrG10H product, the enzyme reaction mixture with microsomal protein extracted from insect cells which were coexpressed with CrG10H and AtCPR1 was analyzed by LC-MS. The product peaks collected from HPLC separation (as described above) were further analyzed by mass spectrometry. Mass spectrometry was carried out on a Finnigan LXQ linear ion trap mass spectrometer (Thermo Finnigan, San Jose, CA) with an electrospray source. Conditions were as follows: electrospray ionization (negative ion mode); the electrospray voltage was set to 4.0 kV; the capillary temperature was 275 °C; the full scan mass spectra of the flavanones

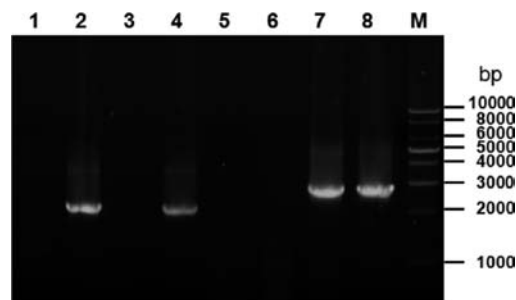


**Figure 2.** PCR analysis of recombinant CrG10H and AtCPR1 in insect cells. Lanes: 1 and 5, untreated insect cells; 2 and 6, insect cells expressing CrG10H; 3 and 7, insect cells expressing AtCPR1; 4 and 8, insect cells coexpressing CrG10H and AtCPR1. CrG10H-S and M13 reverse were used as PCR primers for lanes 1–4 and AtCPR1-S and M13 reverse for lanes 5–8. The migration of DNA markers (M) is shown to the right in base pairs (bp) (Yeastern Biotech Co., Ltd., catalog no. YD001).

from  $m/z$  50 to 300 Da were measured using 500 ms collection time and analyzing three microscans.

## RESULTS AND DISCUSSION

**Gene Cloning and Protein Expression in Sf9 Cells.** We have amplified the CrG10H gene (GenBank accession no. AJ251269) from *C. roseus* and the AtCPR1 gene (GenBank no. X66016) from *A. thaliana* by RT-PCR and expressed them in insect cells using a baculovirus expression system. Heterologous expression using baculovirus vectors has become a popular method for the production of catalytically active P450s.<sup>9,10</sup> We have systematically optimized the multiplicity of infection (MOI) for a coinfection approach for the coexpression of CrG10H and AtCPR1 in Sf9 insect cells. To coexpress the CrG10H and AtCPR1 in Sf9 insect cells, they were individually cloned into pFastBac1 vector, and the resulting target gene was expressed in Sf9 insect cells. The two recombinant baculoviruses were each added at a MOI from 0.25 to 4 (viral titers were determined by the end-point dilution method<sup>11</sup>) and used to infect Sf9 cells at a cell density of  $1 \times 10^6$  cells  $\text{mL}^{-1}$  in SF-900 serum-free medium containing hemin (2  $\mu\text{g mL}^{-1}$ ). The optimal condition for coexpression of CrG10H and AtCPR1 was a fixed MOI value of 1 for recombinant CrG10H and AtCPR1 viruses.

**Coexpression of CrG10H and AtCPR1 in Insect Cells.** PCR analysis was performed to detect CrG10H and AtCPR1 in insect cells. To demonstrate the presence of the CrG10H gene, PCR was performed using CrG10H-S and a second primer M13 reverse located on the bacmid DNA, and the expected product of 2085 bp was obtained (Figure 2, lanes 2 and 4). For detection of AtCPR1, the primer combination AtCPR1-S and M13 reverse was used, giving the expected band of 2682 bp (Figure 2, lanes 7 and 8). Control reactions were performed with each of the above-mentioned primer combinations and DNA prepared from untreated insect cells (Figure 2, lanes 1 and 5). The result showed that CrG10H and AtCPR1 were successfully expressed in insect cells.

**Enzyme Activity Assays.** Recombinant cytochrome P450 was sufficiently expressed in the Sf9 cells such that microsomal protein could be used directly for enzyme assays. Moreover, the recombinant proteins of CrG10H could be detected on the SDS-PAGE gel. A number of substrates were subjected to assay the enzyme activity of CrG10H. As reported in a previous study,<sup>3</sup>

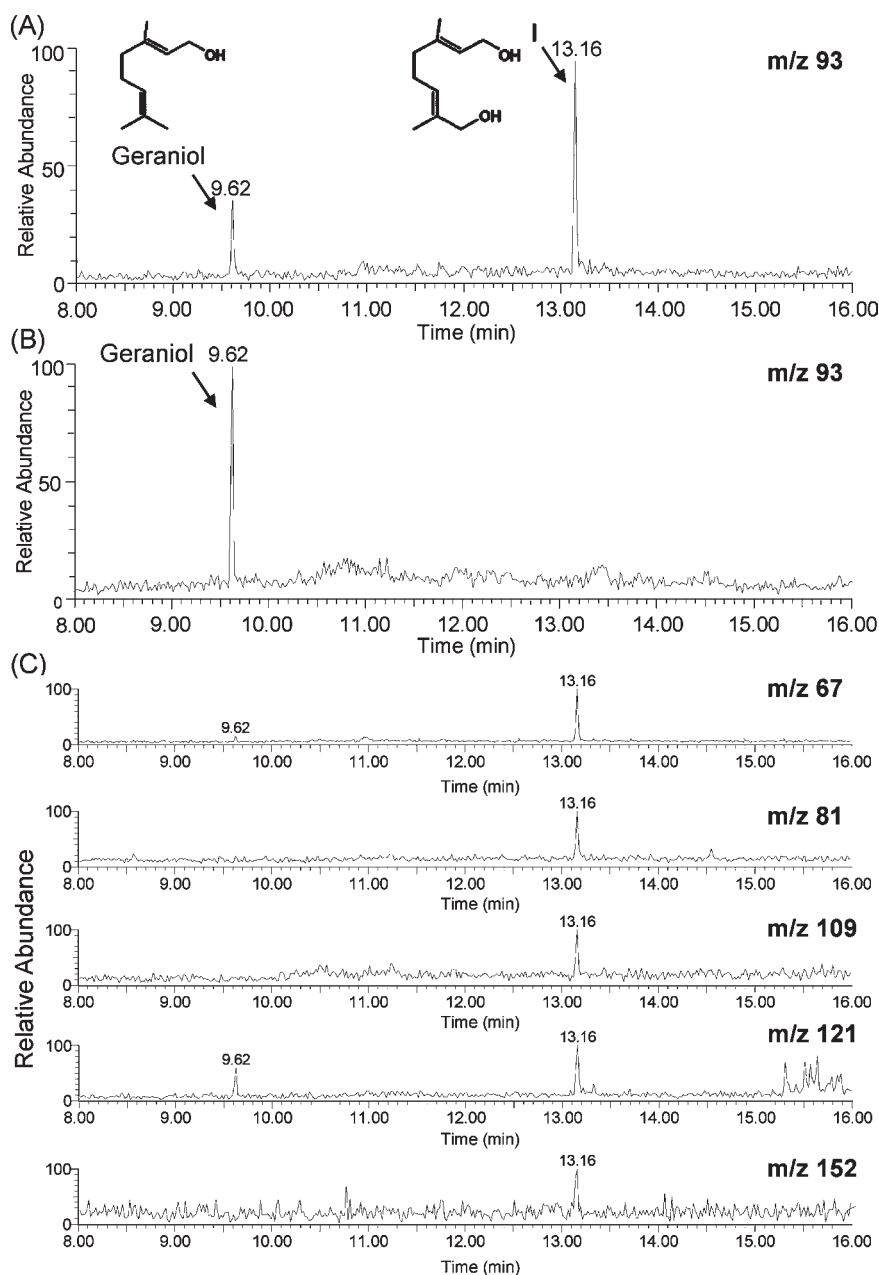


**Figure 3.** GC-MS analysis of the product from the incubation of geraniol with microsomal protein extracted from insect cells coexpressing *CrG10H* and *AtCPR1* (A) or with microsomal protein extracted from untreated control cells (B). Selected ion monitoring (SIM) model  $m/z$  93 was used. (C) Mass spectra analysis of peak I in SIM mode at  $m/z$  67, 81, 109, 121, and 152.

*CrG10H* hydroxylated the monoterpene geraniol at the C-10 position to generate 10-hydroxygeraniol (Figure 3A, peak I). The cells without infection of recombinant virus DNA were used as negative control. No product was detected in the reaction containing microsomal protein extracted from control cells (Figure 3B). Mass spectral analysis and selected ions at  $m/z$  67, 81, 93, 109, 121, and 152 (Figure 3C) positively identified peak I as 10-hydroxygeraniol by comparison with the data reported by Collu et al.<sup>2</sup>

Surprisingly, one product was formed by *CrG10H* when naringenin was used as a substrate (peak II, Figure 4C,D). This compound was not detected in the reactions containing microsomal proteins extracted from untreated control cells or insect cells expressing only *AtCPR1* (Figure 4A,B). The UV spectrum of peak

II (Figure 4E) is shown to be identical to that of authentic eriodictyol (Figure 4F). Furthermore, peak II compound was analyzed by LC-MS. The result showed that the  $MS^2$  ( $m/z$  287→177) and  $MS^3$  ( $m/z$  177→109) fragmentation patterns of the peak II compound were identical to those of authentic eriodictyol. These results indicate that *CrG10H* also catalyzed 3'-hydroxylation of the flavanone naringenin to form eriodictyol. It has been known that the flavonoid 3'-hydroxylase (*F3'H*) also catalyzes the conversion of naringenin to eriodictyol.<sup>12</sup> Comparison of the amino acid sequence of *CrG10H* with those of *F3'H* showed 35–37% identity.

To investigate the biochemical activity of *CrG10H* toward naringenin or geraniol as a substrate, *CrG10H* and *AtCPR1* coexpressed microsomal proteins were used to determine the

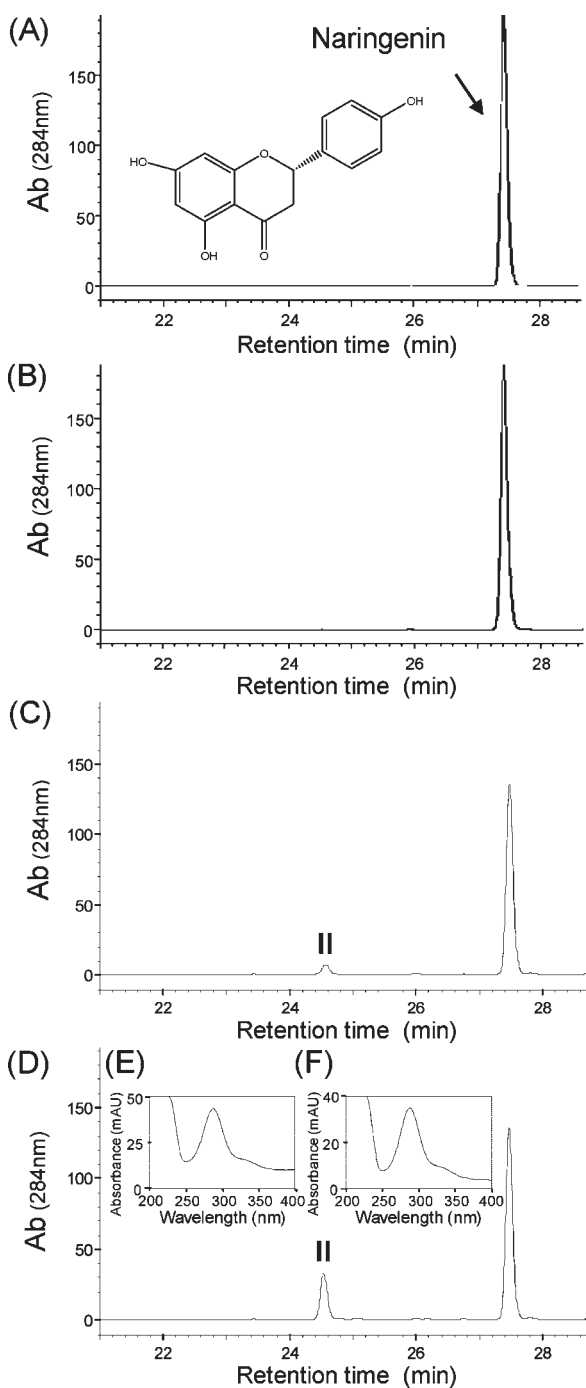


**Figure 4.** HPLC analysis of the product from the incubation of naringenin with microsomal proteins extracted from untreated control cells (A), insect cells expressing *AtCPR1* (B), insect cells expressing *CrG10H* (C), or insect cells coexpressing *CrG10H* and *AtCPR1* (D). The UV spectrum of peak II (E) is shown to be identical to that of authentic eriodictyol (F).

apparent  $K_m$  and  $k_{cat}$  values for these two substrates (Table 1 and Figure 5). The results suggested that *CrG10H* had a better affinity for geraniol than naringenin as determined by their Michaelis constant,  $K_m$ . Judged by the  $k_{cat}/K_m$  values (Table 1), the catalytic activity of *CrG10H* was approximately 10 times more efficient with geraniol than with naringenin. A flavonoid 3',5'-hydroxylase (F3'S'H) has been isolated from *C. roseus*.<sup>13</sup> The *C. roseus* F3'S'H

**Table 1.** Kinetic Parameters for Conversion of Naringenin and Geraniol in the Microsomal Fractions Containing *CrG10H* and *AtCPR1*<sup>a</sup>

substrate	$k_{cat}$ ( $\text{min}^{-1}$ )	$K_m$ ( $\mu\text{M}$ )	$k_{cat}/K_m$ ( $\text{min}^{-1} \mu\text{M}^{-1}$ )
naringenin	$3.15 \pm 0.12$	$58.39 \pm 5.87$	0.054
geraniol	$7.86 \pm 0.75$	$15.81 \pm 3.66$	0.497

<sup>a</sup>The values represent the mean  $\pm$  SD from three separate experiments.

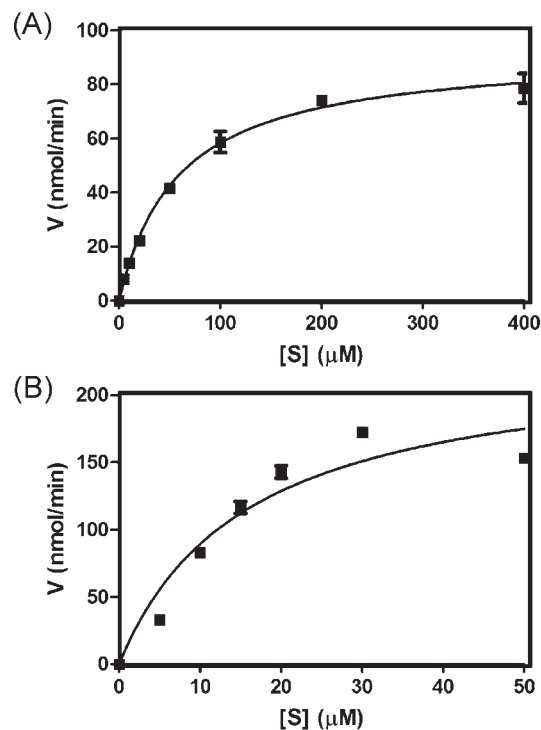


**Figure 5.** Determination of *CrG10H* kinetic constants for naringenin and geraniol. Values are the means of three separate determinations performed at 30 °C using *CrG10H* and *AtCPR1* coexpressed microsomal protein in Tricine buffer (pH 8.0) with various concentrations of naringenin (A) or geraniol (B) and 500  $\mu\text{M}$  NADPH.

also accepted naringenin as a substrate and converted it into both eriodictyol and pentahydroxyflavanone (3'- and 3',5'-hydroxylation). It had an apparent  $K_m$  of 7  $\mu\text{M}$  for naringenin.<sup>13</sup>

Other flavone, flavanone, dihydroflavonol, and flavonol substrates were subjected to assay the enzymatic activity of *CrG10H*, like apigenin, kaempferol, *p*-coumaric acid, and ferulic acid. No reaction products were detected when these substrates were used. *CrG10H* seems to be specific only to naringenin in *C. roseus* flavonoid metabolism. Dihydrokaempferol, which is a substrate for F3'H,<sup>14</sup> was not subjected to assay the enzymatic activity of *CrG10H* because it was not commercially available.

Because cytochrome P450 enzymes depend on associated proteins for their activities, purified or heterologously expressed P450s are usually incorporated into membrane vesicles together with other proteins to measure their activities. The NADPH-cytochrome P450 reductase needs to be incorporated as well, because this protein donates electrons to the cytochrome P450. Our result showed that the catalytic activity of *CrG10H* depended on a plant reductase. Coexpression with *AtCPR1* in insect cells enhanced the 3'-hydroxylation of naringenin to form eriodictyol (Figure 4D). A similar effect was also found by Eugster et al.<sup>15</sup>

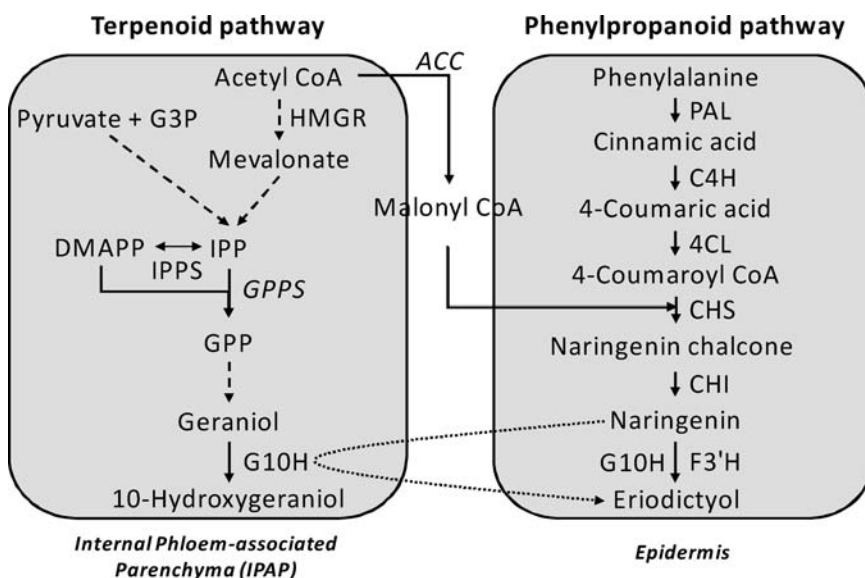


**Figure 6.** Biosynthetic relationships between plant natural products. Thin and dashed arrows represent single and multiple enzymatic steps (based on refs 1 and 2), respectively. The genes involved in the metabolism of terpenoids and flavonoids are in italic type. The right pathway leads to the biosynthesis of flavonoids and the left one to the biosynthesis of isoprenoids. The dotted arrow indicates the proposed translocation of intermediates. PAL, L-phenylalanine ammonia-lyase; C4H, cinnamate 4-hydroxylase; 4CL, 4-coumarate CoA ligase; CHS, chalcone synthase; F3'H, flavonoid 3'-hydroxylase; ACC, acetyl CoA carboxylase; HMGR, 3-hydroxy-3-methylglutaryl CoA reductase; G3P, glyceraldehyde 3-P; IPP, isopentenyl diphosphate; IPSS, IPP isomerase; DMAPP, dimethylallyl diphosphate; GPPS, geranylpyrophosphate synthase; G10H, geraniol 10-hydroxylase.

They succeeded in enhancing the P450-dependent hydroxylation activity by overproduction of a human reductase in yeast. Jennewein et al.<sup>16</sup> also demonstrated significant enhancement of hydroxylase activity when a plant reductase was coexpressed along with the taxoid 10-hydroxylase in yeast.

The monoterpenoid pathway exhibits a complex multicellular organization that has been extensively characterized in *C. roseus* and is now cited as an example of the extraordinarily complex spatial organization that plants sometimes develop to accomplish their secondary metabolisms. In planta, secondary metabolisms are spatially and temporally regulated, depending on highly differentiated tissues or cells. The early steps of monoterpenoid biosynthesis catalyzed by 1-deoxy-D-xylulose 5-phosphate (DXP) synthase, DXP reductoisomerase, 2C-methyl-D-erythritol 2,4-cyclodiphosphate synthase, hydroxymethylbutenyl 4-diphosphate synthase, and G10H were suggested to take place in the internal phloem-associated parenchyma (IPAP) cells, whereas flavonoids accumulate in the epidermal cells.<sup>17–19</sup> Recent data from in situ RNA hybridization and RT-PCR analysis suggest that the *G10H* mRNA was expressed in both IPAP<sup>20,21</sup> and epidermis<sup>17,21</sup> of *C. roseus*. This is direct evidence supporting the dual multicellular localization of G10H. However, the IPAP has been proposed as a major site of precursor biosynthesis, and G10H is involved in the first committed step in the terpenoid pathway in *C. roseus*.<sup>20</sup> It is not clear if G10H expressed in the IPAP cells can be mobilized to the leaf epidermal cells for biosynthesis of flavonoids. We predict that the translocation of pathway intermediates from the epidermis to IPAP during phenylpropanoid synthesis would be more reasonable (Figure 6). A similar cell-type specific expression of F3'S'H, which modifies naringenin with additional hydroxylations on the B-ring, was present in the internal phloem of *C. roseus*.<sup>13</sup> However, genes involved in flavonoid biosynthesis were expressed preferentially in the epidermis.<sup>13,18</sup> Therefore, it is possible that CrG10H, although located in the IPAP, takes part in the hydroxylation of naringenin on the B-ring.

It has been known that G10H hydroxylates the monoterpene geraniol at the C-10 position to produce 10-hydroxygeraniol.<sup>2,3,22,23</sup> This reaction is the key step for the biosynthesis of TIAs. In our study, we demonstrate that G10H from *C. roseus* also catalyzes 3'-hydroxylation of naringenin to produce eriodictyol. This is the first paper to describe the additional function of G10H involved in the biosynthetic pathway of flavonoids in vitro. We believe that G10H plays an important role in both terpenoid and flavonoid metabolism. To further clarify the role and function of G10H in vivo, it would be necessary to determine the nature and concentrations of the flavonoids present and to compare the substrate specificities in *C. roseus*.

## AUTHOR INFORMATION

### Corresponding Author

\*(P.-L.H.) Phone: +886-2-33664836. Fax: +886-2-23627053. E-mail: pungling@ntu.edu.tw. (Y.-Y.D.) Phone & Fax: +886-2-33664835 +886-2-33664835. E-mail: yiyindo@ntu.edu.tw.

### Present Addresses

<sup>5</sup>Biotechnology of Natural Products, Technical University München, Liesel-Beckmann-Str. 1, 85354 Freising, Germany.

### Author Contributions

<sup>||</sup>Contributed equally to this work.

## ACKNOWLEDGMENT

We thank Professor Ting-Jang Lu (Institute of Food Science and Technology, NTU, Taiwan) and Dr. Jeng-Der Chung (Taiwan Forestry Research Institute, Taiwan) for their technical assistance with MS analysis. We thank Dr. Raghu Rajasekaran for a critical reading of the manuscript.

## REFERENCES

- (1) Hughes, E. H.; Hong, S. B.; Gibson, S. I.; Shanks, J. V.; San, K. Y. Metabolic engineering of the indole pathway in *Catharanthus roseus* hairy roots and increased accumulation of tryptamine and serpentine. *Metab. Eng.* **2004**, *6*, 268–276.
- (2) Collu, G.; Garcia, A. A.; van der Heijden, R.; Verpoorte, R. Activity of the cytochrome P450 enzyme geraniol 10-hydroxylase and alkaloid production in plant cell cultures. *Plant Sci.* **2002**, *162*, 165–172.
- (3) Collu, G.; Unver, N.; Peltenburg-Looman, A. M. G.; van der Heijden, R.; Verpoorte, R.; Memelink, J. Geraniol 10-hydroxylase, a cytochrome P450 enzyme involved in terpenoid indole alkaloid biosynthesis. *FEBS Lett.* **2001**, *508*, 215–220.
- (4) Suttipanta, N.; Pattanaik, S.; Gunjan, S.; Xie, C. H.; Littleton, J.; Yuan, L. Promoter analysis of the *Catharanthus roseus* geraniol 10-hydroxylase gene involved in terpenoid indole alkaloid biosynthesis. *Biochim. Biophys. Acta* **2007**, *1769*, 139–148.
- (5) Porter, T. D.; Wilson, T. E.; Kasper, C. B. Expression of a functional 78,000 Da mammalian flavoprotein, NADPH-cytochrome P-450 oxidoreductase, in *Escherichia coli*. *Arch. Biochem. Biophys.* **1987**, *254*, 353–367.
- (6) Schuler, M. A.; Werck-Reichhart, D. Functional genomics of P450s. *Annu. Rev. Plant Biol.* **2003**, *54*, 629–667.
- (7) Kraus, P. F. X.; Kutchan, T. M. Molecular cloning and heterologous expression of a cDNA encoding berbaminine synthase, a C–O phenol-coupling cytochrome P-450 from the higher plant *Berberis stolonifera*. *Proc. Natl. Acad. Sci. U.S.A.* **1995**, *92*, 2071–2075.
- (8) Omura, T.; Sato, R. The carbon monoxide-binding pigment of liver microsomes: I. Evidence for its hemoprotein nature. *J. Biol. Chem.* **1964**, *239*, 2370–2378.
- (9) Chen, L.; Buters, J. T. M.; Hardwick, J. P.; Tamura, S.; Penman, B. W.; Gonzalez, F. J.; Crespi, C. L. Co-expression of cytochrome P450A6 and human NADPH-P450 oxidoreductase in the baculovirus system. *Drug. Metab. Dispos.* **1997**, *25*, 399–405.
- (10) Ohnishi, T.; Bancos, S.; Watanabe, B.; Fujita, S.; Szatmari, M.; Koncz, C.; Lafos, M.; Yokota, T.; Sakata, K.; Szekeres, M.; Mizutani, M. C-23 hydroxylation by *Arabidopsis* CYP90C1 and CYP90D1 reveals a new shortcut route in brassinosteroid biosynthesis. *Plant Cell* **2006**, *18*, 3275–3288.
- (11) O'Reill, D. R.; Miller, L. K.; Luckow, V. A. *Baculovirus Expression Vectors, A Laboratory Manual*; Freeman: New York, 1992.
- (12) Schoenbohm, C.; Martens, S.; Eder, C.; Forkmann, G.; Weisshaar, B. Identification of the *Arabidopsis thaliana* flavonoid 3'-hydroxylase gene and functional expression of the encoded P450 enzyme. *Biol. Chem.* **2000**, *381*, 749–753.
- (13) Kaltenbach, M.; Schröder, G.; Schmelzer, E.; Lutz, V.; Schröder, J. Flavonoid hydroxylase from *Catharanthus roseus*: cDNA, heterologous expression, enzyme properties and cell-type specific expression in plants. *Plant J.* **1999**, *19*, 183–193.
- (14) Forkmann, G. Flavonoids as flower pigments: the formation of the natural spectrum and its extension by genetic engineering. *Plant Breed.* **1991**, *106*, 1–26.
- (15) Eugster, H. P.; Bärtsch, S.; Würigler, F. E.; Sengstag, C. Functional co-expression of human oxidoreductase and cytochrome P450 1A1 in *Saccharomyces cerevisiae* results in increased EROD activity. *Biochem. Biophys. Res. Commun.* **1992**, *185*, 641–647.
- (16) Jennewein, S.; Park, H.; DeJong, J. M.; Long, R. M.; Arthur, P. B.; Croteau, R. B. Coexpression in yeast of *Taxus* cytochrome P450 reductase with cytochrome P450 oxygenases involved in taxol biosynthesis. *Biotechnol. Bioeng.* **2005**, *89*, 588–598.
- (17) Oudin, A.; Mahroug, S.; Courdavault, V.; Hervouet, N.; Zelwer, C.; Rodriguez-Concepcion, M.; St-Pierre, B.; Burlat, V. Spatial distribution and hormonal regulation of gene products from methyl erythritol phosphate and monoterpene-secoiridoid pathways in *Catharanthus roseus*. *Plant Mol. Biol.* **2007**, *65*, 13–30.
- (18) Murata, J.; Roepke, J.; Gordon, H.; De Luca, V. The leaf epidermome of *Catharanthus roseus* reveals its biochemical specialization. *Plant Cell* **2008**, *20*, 524–542.
- (19) Guirimand, G.; Burlat, V.; Oudin, A.; Lanoue, A.; St-Pierre, B.; Courdavault, V. Optimization of the transient transformation of *Catharanthus roseus* cells by particle bombardment and its application to the subcellular localization of hydroxymethylbutenyl 4-diphosphate synthase and geraniol 10-hydroxylase. *Plant Cell Rep.* **2009**, *28*, 1215–1234.
- (20) Burlat, V.; Oudin, A.; Courtois, M.; Rideau, M.; St-Pierre, B. Co-expression of three MEP pathway genes and geraniol 10-hydroxylase in internal phloem parenchyma of *Catharanthus roseus* implicates multicellular translocation of intermediates during the biosynthesis of monoterpene indole alkaloids and isoprenoid-derived primary metabolites. *Plant J.* **2004**, *38*, 131–141.
- (21) Murata, J.; De Luca, V. Localization of tabersonine 16-hydroxylase and 16-OH tabersonine-16-O-methyltransferase to leaf epidermal cells defines them as a major site of precursor biosynthesis in the vindoline pathway in *Catharanthus roseus*. *Plant J.* **2005**, *44*, 581–594.
- (22) Dixon, R. A. Natural products and plant disease resistance. *Nature* **2001**, *411*, 843–847.
- (23) Leonard, E.; Yan, Y.; Koffas, M. A. Functional expression of a P450 flavonoid hydroxylase for the biosynthesis of plant-specific hydroxylated flavonols in *Escherichia coli*. *Metab. Eng.* **2006**, *8*, 172–181.